Aeroelastic Modelling and Comparison of Advanced Active Flap Control Concepts for Load Reduction on the Upwind 5MW Wind Turbine

T.K. Barlas[1] and G.A.M. van Kuik[2]

DUWIND, Delft University of Technology, Kluyverweg 1, Delft, Netherlands.
[1] a.barlas@tudelft.nl
[2] g.a.m.vankuik@tudelft.nl

Abstract

A newly developed comprehensive aeroelastic model is used to investigate active flap concepts on the Upwind 5MW reference wind turbine. The model is specially designed to facilitate distributed control concepts and advanced controller design. Different concepts of centralized and distributed control schemes based on choices of realistic measurement signals are compared. The sensitivity of important parameters to the load reduction capability is investigated and main differences between control approaches are analyzed. Conclusions are drawn regarding optimal integration of active flaps on wind turbines. Research work is performed at Delft University Wind Energy Research Institute (DUWIND), funded by EU's FP6 project "UPWIND".

Nomenclature

Cl: lift coefficient
Cm: pitching moment coefficient
Ch: flap hinge moment coefficient
b: airfoil semi-chord [m]
V: wind speed [m/s]
h: plunge amplitude [m]
α: angle of attack [rad]
a: dimensionless pitch axis location
F: geometric constants for flap
α_{qs}: quasi-steady angle of attack [rad]
δ_{qs}: quasi-steady angle of attack due to flap deflection [rad]
wg: vertical gust field velocity [m/s]
z: aerodynamic lag states
IEC: International Electrotechnical Commitie
SISO: Single Input Single Output
MIMO: Multiple Input Multiple Output
CFD: Computational Fluid Dynamics
IFC: Individual Flap Control
MFC: Multiple Flap Control
HSS: High Speed Shaft

Introduction - Motivation

Reducing loads on wind turbine rotors can offer large reduction in the cost of energy, by affecting both the capital and maintenance costs. With the increasing size of wind turbine

blades, the need for more sophisticated load control techniques has induced interest in locally distributed aerodynamic control systems with build-in intelligence on the blades (often referred to in popular terms as 'smart structures' or 'smart rotor control'). A review of concepts, feasibility and inventory of design options for such systems has been performed by Barlas and van Kuik [1]. Active load control through trailing edge flaps or deformable trailing edge geometry is considered a feasible and efficient solution, because of the direct lift control capability and the advances in smart material actuator technology.

Previous work with CFD (see Troldborg [2]), 2D aeroelastic models (see [3], [4], [5]) and BEM-based or Vortex-based aeroelastic models (see Andersen et al [6] and Riziotis and Voutsinas [7]), has shown the potential of applying active control through flaps or variable geometry trailing edge airfoils on wind turbine blades for load reduction purposes. Also, wind tunnel tests have been used to quantify unsteady aerodynamics responses and aerodynamic load reductions (see Bak et al [8]) and prove the concept of active flaps for feedback load control on scaled aeroelastic models (see van Wingerden et al [9] and Barlas et al [10]). As the concepts become more mature, more integrated studies are performed taking all operating conditions into account, combining the flap control schemes with the existing controls. In this case, specific control concepts are utilized and the combination of power regulation and load reduction controllers is investigated (see Andersen et al [11]).
There are various options for utilizing active flaps which operate locally along the blade span for load reduction. In order to establish the maximum load reduction potential for every concept and identify the most realistic and cost effective solutions, all options should be compared on an equal basis and in a standard integrated control design approach. This article presents such a comparison of distributed and centralized control concepts, based on different measured signals, utilizing traditional controller design methods. First, the newly developed aeroelastic model is presented. All the extended modules to facilitate various distributed control concepts are described. Next, the blade load control reduction in IEC standard power production normal turbulence load cases is shown for different control approaches. Conclusions are drawn.

Description of numerical model

In Delft University Wind Energy Research Institute (DUWIND) a comprehensive aeroservoelastic tool has been developed. Although a variety of widely used aeroelastic codes are available for design, certification and research purposes, the new code has been developed in order to have the advantage of a modular structure, to be able to incorporate realistic effects of distributed trailing edge flaps and to allow for rapid and easy design and implementation of real time controllers. This led to the development of DU_SWAMP (Delft University Smart Windturbine Aeroelastic Modular Processing). The code is implemented in Matlab$^{©}$ Simulink$^{©}$ and comprises a full aeroservoelastic wind turbine model, extended with distributed active control capability blade features. The structure of the code is fully modular, which offers the possibility to easily adapt the model configuration and complexity by interchanging modules (Fig. 1). The implementation of additional features like trailing edge flap aerodynamics models or actuator dynamics behavior is thus facilitated. The model layout also offers the opportunity to use model linearization, system identification and various controller design tools utilizing any available signal in the model. Innovative feedback or feed-forward control schemes based on single-input-single-output (SISO) or multiple-input-multiple-output (MIMO) schemes are easily implemented.
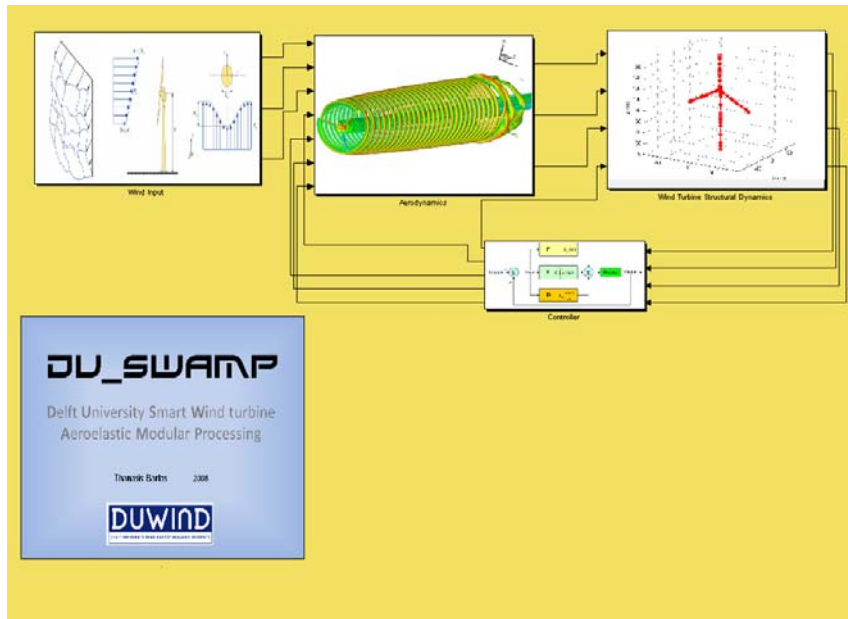
Fig. 1: *The Simulink$^{©}$ graphical interface showing sub-modules of DU_SWAMP*

The rotor aerodynamics submodel consists of a multiple-streamtube Blade Element representation coupled with a dynamic inflow model (as described by Snel [12] for the unsteady wake induction. The sectional aerodynamics are described by 2d tabulated data, corrected for 3d effects (using the Viterna method). For the case of the flapped sections a 2d unsteady aerodynamic model is used, based on work for helicopters, as described by Leishman (see [13] and [14]). The model analytically predicts the aerodynamic responses of a thin airfoil to arbitrary forcing inputs (airfoil motion, gusts, flap deflection) through an indicial response formulation. Thus, the dynamic effect of a flap actuation is realistically simulated. In fact, the analytical state-space solution is a different representation of the Theodorsen and Wagner function in the time domain (see Theodorsen [15], Wagner [16] and Bisplinghoff [17]). The model is valid for attached flow conditions. Since the model has been adapted for wind turbine applications, the general theoretical background is explained here. The calculated unsteady Cl, Cm and Ch is comprised of the non-circulatory part (due to the acceleration of the airfoil in the fluid, [Eq. 2]), which can be calculated directly by the instantaneous values and rates of the motions, and the circulatory part (due to the influence of the shed vorticity), [Eq. 3]), which causes both an amplitude change and a phase change (lead or lag) in the response. The circulatory part is calculated by superimposing the effect of all the forcing inputs. These effects are estimated by the use of Duhamel superposition integral, so actually calculating the response to an arbitrary input when the response to an indicial (step) input is known. The indicial responses for thin airfoils are known from theory (e.g. [16]) or can be derived from wind tunnel measurements or CFD. For the airfoil or trailing edge flap motion the response is given by the Wagner function. This is the same for airfoil motion or trailing edge flap deflection, since the circulatory lift lag is an intrinsic function of the fluid and does not depend on the airfoil boundary conditions [13]. On the other hand the Küssner function is used for the indicial response to a sharp vertical gust field (the disturbances in the wind speed in this case). For practical reasons, both functions can be replaced by exponential approximations. Once the indicial responses are know, the impulsive responses can be calculated. The transfer function of the lag system can be calculated by taking the Laplace transform of the impulsive responses. This transfer function can be easily put in controllable canonical (state-space) form ([Eq. 4] and [Eq. 5]). The parameters in the A, B, C, D matrices are evaluated from the exponential approximations of the Wagner and Küssner functions. All effects of forcing functions can be combined in one state-space system (with the aerodynamic lag states being z, as many as the forcing functions), making the evaluation of the circulatory part of the Cl computationally efficient. The state-space form is also practical for implementation into aeroelastic models and especially for control design. The full aerodynamic system can be represented by 4 states (2 for arbitrary airfoil and

flap motion and 2 for the gust field). The unsteady Cm and Ch can be calculated similarly, with equivalent formulations for the non-circulatory and circulatory parts.

$$C_L = C_L^{nc} + C_L^c \qquad \text{(Eq. 1)}$$

$$C_L^{nc} = \frac{\pi b}{V^2}\left(\dot{h} + V\dot{\alpha} - ba\ddot{\alpha}\right) + \frac{b}{V^2}\left(-VF_4\dot{\delta} - bF_1\ddot{\delta}\right) \text{(Eq. 2)}$$

$$C_L^c = \left(C_L^c\right)_\alpha + \left(C_L^c\right)_\delta + \left(C_L^c\right)_{wg} \qquad \text{(Eq. 3)}$$

$$\begin{Bmatrix} \dot{z}_1 \\ \dot{z}_2 \\ \dot{z}_3 \\ \dot{z}_4 \end{Bmatrix} = [A]\begin{Bmatrix} z_1 \\ z_2 \\ z_3 \\ z_4 \end{Bmatrix} + [B]\begin{Bmatrix} \alpha_{qs} + \delta_{qs} \\ \dfrac{wg}{V} \end{Bmatrix} \qquad \text{(Eq. 4)}$$

$$(C_L^c)_{\alpha,\delta,wg} = [C]\begin{Bmatrix} z_1 \\ z_2 \\ z_3 \\ z_4 \end{Bmatrix} + [D]\left(\alpha_{qs} + \delta_{qs}\right) \text{(Eq. 5)}$$

The wind input sub-model contains all the required wind disturbance effects according to IEC, including wind shear, tower shadow and turbulence. Wind files are generated and used during simulation. A roughness length of 0.03 is used in the wind shear model in the simulations presented. The turbulence intensity is determined for every simulated average wind speed, according to IEC for a class 1B wind turbine. Arbitrary wind inputs can be easily simulated, which is necessary, for example, for system identification input excitations or extreme wind load cases.

The structural dynamics sub-model of the wind turbine is aeroelastically coupled to the aerodynamic model, by means of the structural deformation velocities and the aerodynamic forces. It consists of a hybrid multi body representation of the wind turbine components. The main flexible structural components (i.e. blades and tower) are represented by superelements (i.e. sets of non-equally distributed rigid bodies connected with linear springs and dampers, see Fig. 2). These are connected with other rigid bodies to formulate the full wind turbine multi-body structural problem. The concept of superelements is considered more accurate and computationally efficient than the concept of `lumped-masses' (see Molenaar [18], Holierhoek [19] Shabana [20] and Rauh and Sciehlen [21]). In this way non-linear deflections can also be simulated. All necessary blade degrees of freedom are included (flap-wise bending, edgewise bending and torsion). The total number of degrees of freedom in the full wind turbine configuration is determined by the number of superelements used per flexible body. In order to capture the first two bending modes of blades and tower, two to three superelements are used, leading to 40 to 60 degrees of freedom in the full wind turbine configuration. No drivetrain dynamics are simulated, and the gearbox is represented by a simple gearbox ratio of 97. The sum of losses in the drivetrain and generator is 5.6%.

The baseline controllers of the wind turbine are included for power regulation, i.e. generator torque control and above rated full-span pitch control. Any addition of other kind of load reduction controller is facilitated, like cyclic or individual pitch control, individual flap control (one flap per blade) or distributed flap control. Virtually any signal can be used for controller input. In the analysis presented here, realistic sensor signals are used. The actuator dynamics can also be specified in detail, by means of transfer functions, low order dynamic systems, or by setting

saturation limits and rate limits for the actuation. This allows for detailed modeling of smart-material based actuation, which has an important contribution to the dynamics of the full model.
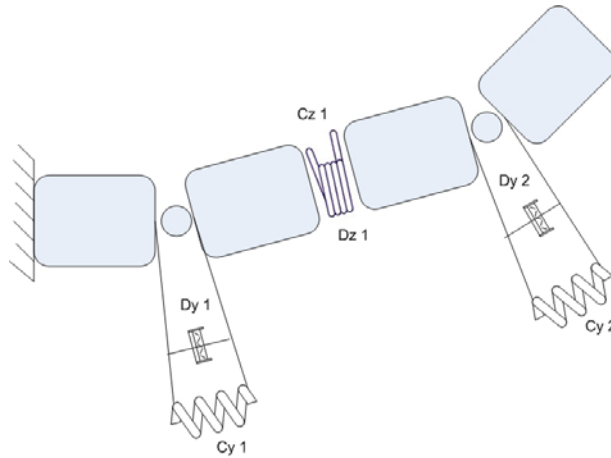

Fig. 2: *Superelement representation*

Controller design and simulations

The Upwind/NREL 5MW reference wind turbine is used as a baseline for all simulations (see [22]). The properties and operating conditions of the reference wind turbine are summarized in Table 1.

Rated power	5	MW
Wind Regime	IEC Class 1B / Class 6 winds	
Rotor Orientation	Clockwise rotation - Upwind	
Control	Variable Speed, Collective pitch	
Cut in wind speed	4	m/s
Cut out wind speed	25	m/s
Number of blades	3	
Rotor Diameter	126	m
Hub Diameter	3	m
Hub Height	90	m
Maximum Rotor Speed	12.1	rpm
Maximum Generator Speed	1,173.7	rpm
Gearbox Ratio	97.0	-
Maximum Tip Speed	80.0	m/s
Hub Overhang	5.0	m
Shaft Tilt Angle	5.0	°
Rotor Precone Angle	-2.5	°
Rotor Delta3 (sweep) Angle	0.0	°
Blades mass (All)	53,220	kg
Hub mass	56,780	kg
Rotor (Blades + Hub) mass	110,000	kg
Nacelle mass	240,000	kg
Tower + Monopile (Support Shallow) mass	522,617	kg
Overall mass	872,617	kg
Blade structural damping ratio	0.47	%
Tower structural damping ratio	1	%

Table 1: General characteristics of the Upwind 5MW Reference Wind Turbine

The baseline configuration of the model has been verified against simulation data with other commercial codes at representative operating conditions. Next, this configuration is updated to include the control capability of active flaps on the blades. Three main global load control strategies are considered and are investigated:

- *Decentralized individual flap control* (Fig. 3)
  One large flap per blade is used. Each flap reacts on the same blade's flapping root moment based on a feedback control rule. All three single-input-single-output (SISO) feedback loops are decoupled, thus this control scheme is referred to as decentralized

- *Centralized individual flap control* (Fig. 4)
  One large flap per blade is used. A multi-blade rotational transformation technique is used to transform blade root flapping moments into rotor yaw and tilt moments [22]. This results in two decoupled SISO feedback loops. A third SISO loop can be used to impose a collective flap angle, used additionally for power regulation. Since the three individual flaps are control based on global rotor signals (in fixed reference frame), this control scheme is referred to as centralized.

- *Decentralized multiple feedback flap control (Fig. 5)*
  Multiple flaps per blade are used. Each flap is activated based on local flapwise deformation signals via a feedback rule. All SISO loops are fully decoupled.
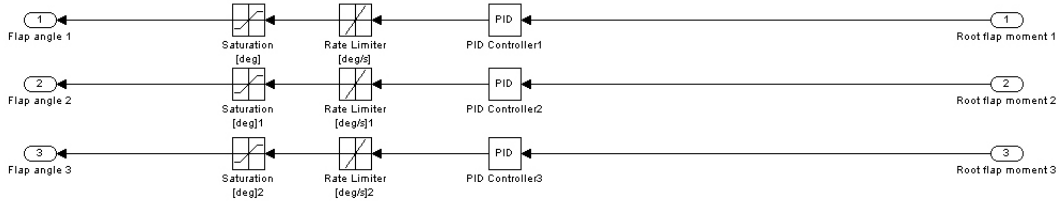

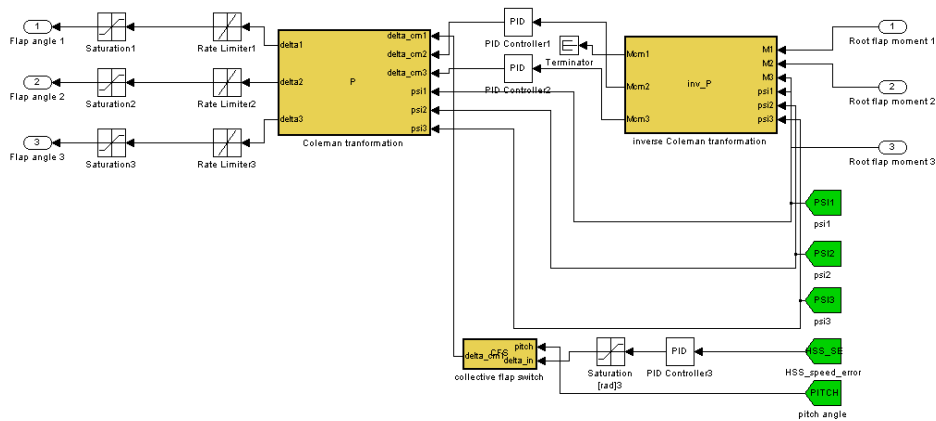Fig. 3: *Decentralized individual flaps control scheme.*

Fig. 4: *Centralized individual flaps control scheme (incl. Coleman transformation).*

For every case, representative operating wind speeds are chosen (8, 11.4 and 16 m/s), covering below and above rated wind speed operation. The baseline controllers for power regulation (i.e. generator torque control and above rated collective pitch) are used normally in every case, based on original design of Jonkman [23] and the implementation of Namic in Simulink[©] [24]. They consist of a multi-region torque controller (Fig. 6), where the generator torque is given by a square function of the high speed shaft (HSS) rotational speed at region 2,

whereas is calculated as rated power over HSS speed at region 3 (above rated). Linear slope regions 1.5 and 2.5 are also included for the transient operation between the regions. The HSS speed is filtered with a low pass filter at 0.25 Hz in order to avoid aggressive response of the torque and pitch controller to high frequency vibrations at the shaft.
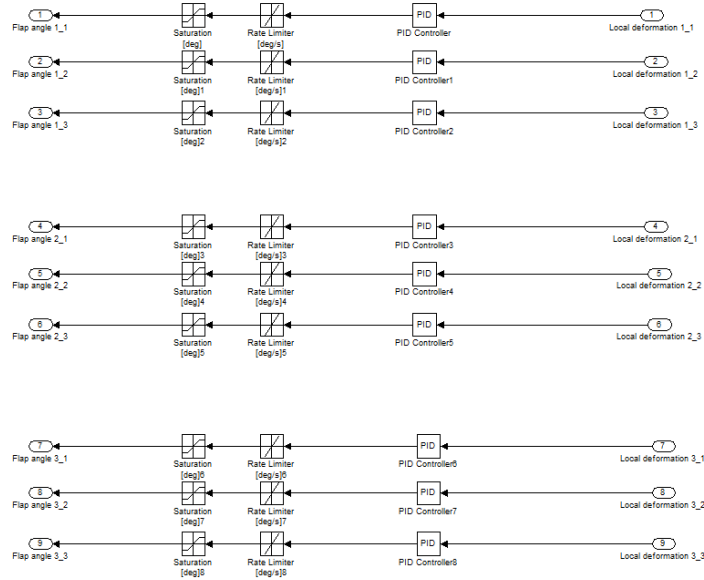

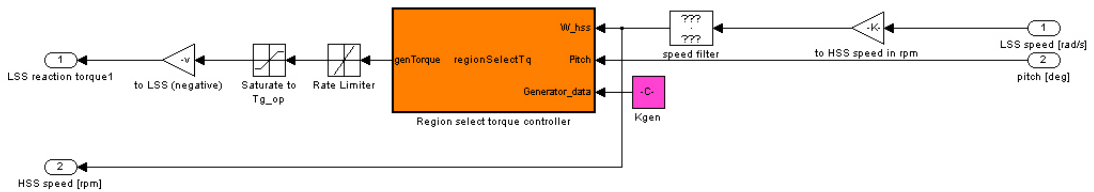Fig. 5: *Decentralized multiple flap controller scheme*

Fig. 6: *Generator torque controller scheme.*

The collective pitch angle is determined via a PI feedback control loop based on the filtered HSS speed (Fig. 7). The gains are scheduled for every operating point, based on the pitch angle using the function:

$$GS(\theta) = \frac{1}{1 + \dfrac{\theta}{\theta_k}}$$ (Eq. 6)
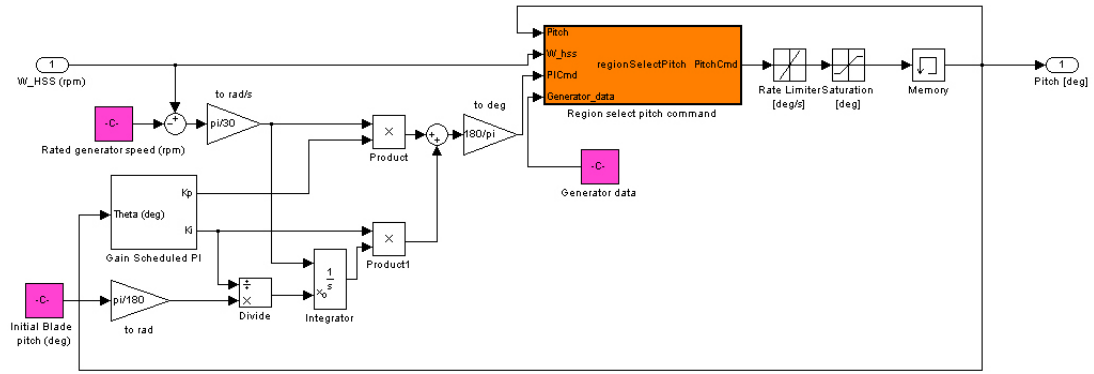
Fig. 6: *Collective pitch controller scheme.*

For all cases and concepts investigated, the controller design is performed using traditional linear control theory. A linear state-space model of the aeroservoelastic system (open loop from the actuator to the measurement signal in every case) is extracted using numerical perturbation linearization of the non-linear plant, utilizing Simulink tools [see 25]. The full non-linear model is written in state-space form:

$$\dot{x}(t) = f\left(x(t)u(t),t\right)$$
$$y(t) = g\left(x(t)u(t),t\right)$$

(Eq 7.)

The linearized version of the model, which is valid around the chosen operating point defined by certain inputs, states and outputs, can be written in terms of the perturbation variables:

$$\delta\dot{x}(t) = A\delta x(t) + B\delta u(t)$$
$$\delta y(t) = C\delta x(t) + D\delta u(t)$$

(Eq. 8)

To compute the matrices, the states and inputs are perturbed, one at a time, and the response of the system to this perturbation is measured by computing $\delta\dot{x}$ and δy. The perturbation and response are then used to compute the matrices in the following way:

$$A(:,i) = \frac{\dot{x}\big|_{x_{p,i}} - \dot{x}_o}{x_{p,i} - x_o}, \qquad B(:,i) = \frac{\dot{x}\big|_{u_{p,i}} - \dot{x}_o}{u_{p,i} - u_o}$$

$$C(:,i) = \frac{y\big|_{x_{p,i}} - y_o}{x_{p,i} - x_o}, \qquad D(:,i) = \frac{y\big|_{u_{p,i}} - y_o}{u_{p,i} - u_o}$$

(Eq. 9)

The linearized models are computed around each relevant operating point, in an averaged way, in order to eliminate periodic effects. The models obtained are analyzed in terms of frequency response, and a PID controller is designed using classical control methods with the target of minimizing the fluctuations in the required signal in every case (blade root flapwise bending moment, tip acceleration, local accelerations). Additional lowpass filters are also used in order to suppress unwanted high frequencies. System identification methods have also been explored in order to derive the state-space model, but were not utilized in the results presented here.

Results

The concepts are compared in terms of fatigue load reduction performance, primarily quantified with the standard deviation of flapwise blade root bending moment. Every case is analyzed in order to determine the physical basis that drives the differences in performance. Conclusions are drawn about the optimization of the integration of active flaps on wind turbine blades, considering realistic design options.

In the Individual Flap Control cases, one big flap of 20% blade spanwise length is used. The flaps occupy 10% of the chordwise length in every used section. The allowed flap angles (saturation limits) are ±10 degrees and the maximum flap rate is ±40 degrees per second, corresponding to realistic performance of actuators based on smart materials or compliant mechanism structures. In the Multiple Flap Control case, the same area of flap is used (20%R), split into three parts. Local flapwise deformation signals are used as inputs to the controller. The main results from the IEC standard power production normal turbulence load cases can be seen below.

The time series results from the decentralized IFC are shown in Fig. 7. We see the activity of each flap on every blade using the designed feedback control law based on each blade's flapwise root moment. A considerable reduction in both the standard deviation of the flapwise root moment and flapwise tip deflection is achieved. The perodicity of the system, especially around the rotor frequency (1p) can be seen together with the appropriate flap response.
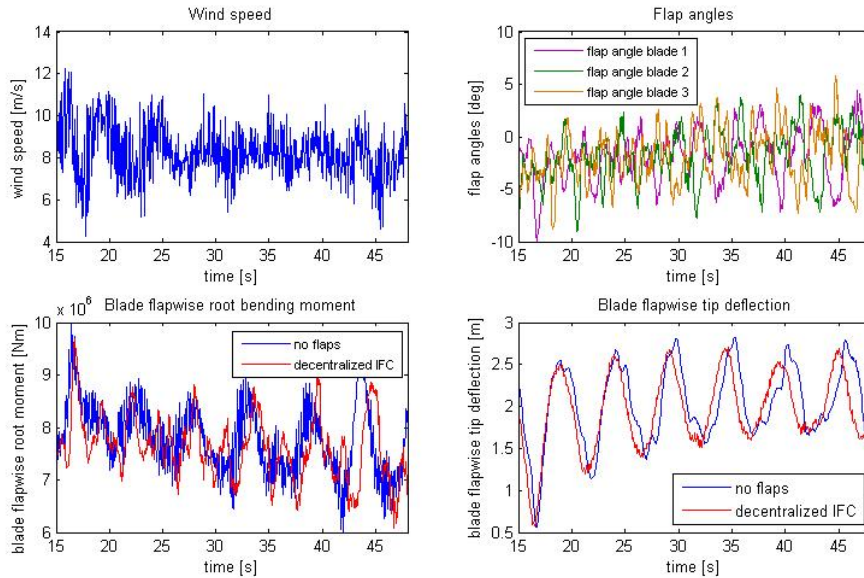

Fig. 7: *Time series with Decentralized Individual Flap Control*

The time series results from the centralized IFC are shown in Fig. 8. In this case, the flaps react based on the designed feedback control law, in order to alleviate fluctuations in the rotor tilt and yaw moments. A considerable reduction in both the standard deviation of the flapwise root moment and flapwise tip deflection is achieved. The results compare well with the ones presented in [22] considering the differences in the used models. It should be noted, that even after the Coleman transformation the system is still periodic in nature, something that is seen also during linearization. For a detailed discussion on this issue, see [26] and [27].
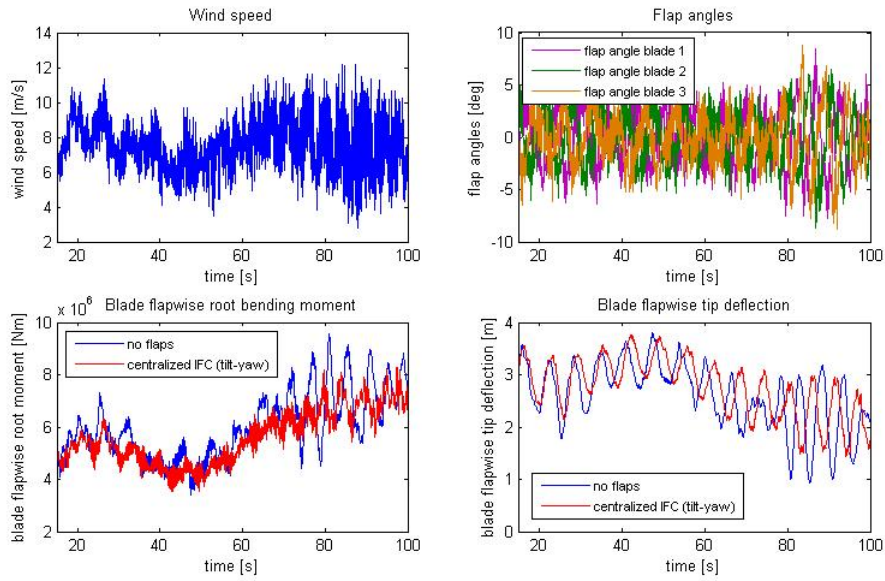
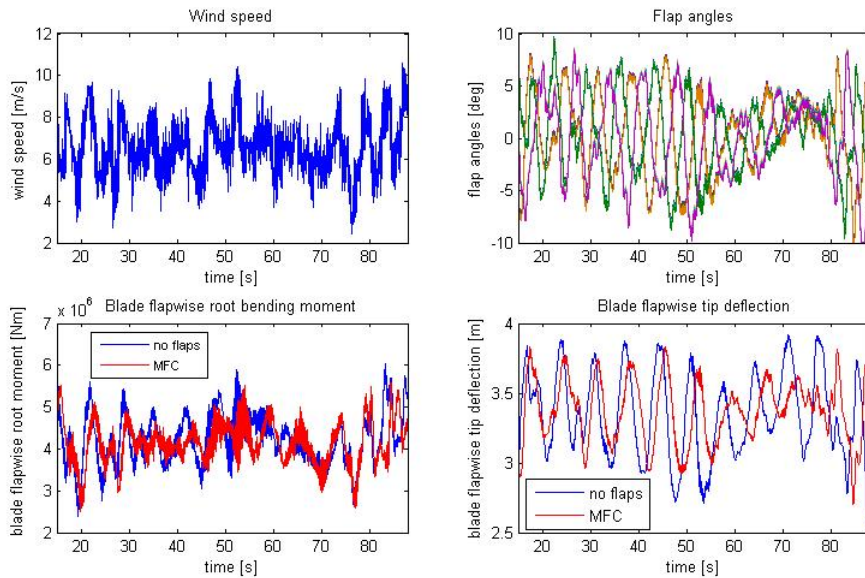Fig. 8: *Time series with Centralized Individual Flap Control (Coleman or 'tilt-yaw')*

Fig. 9: *Time series with Decentralized Multiple Flap Control*

The time series results from the deccentralized MFC are shown in Fig. 9. In this case, the three flaps per blade react independently based on the designed feedback control law, in order to alleviate fluctuations in the local flapwise deformations. A considerable reduction in both the standard deviation of the flapwise root moment and flapwise tip deflection is achieved.

In all the cases, a reduction in the standard deviation of the collective pitch angle was also achieved, since the reduction in fluctuating loads at low frequencies also helps in regulating the rotor speed. On the other hand, a slight decrease in mean power was observed, something that has been discussed also in other relevant publications (see [11] and [22]). No particular effort has been put in modifying the control law to compensate for that, although the possibility has been verified. Results for all investigated load cases are compiled in table 2.

control scheme		IFC			IFC-Coleman			MFC	
average wind speed	8 m/s	11.4 m/s	18 m/s	8 m/s	11.4 m/s	18 m/s	8 m/s	11.4 m/s	18 m/s
flap root moment std	15.41	10.23	17.32	9.26	5.78	7.92	19.32	16.35	22.41
flap tip deflection std	9.26	5.54	10.21	8.01	2.61	1.91	31.01	20.54	34.52
FA tower root moment	4.31	3.67	5.01	3.47	8.99	1.47	17.25	15.56	18.33
FA tower top deflection	3.98	3.02	4.13	4.49	9.24	0.97	15.93	13.21	16.02
Mean generator power	-0.89	-0.53	-0.45	-1.22	-0.32	-0.14	-0.88	-0.61	-0.54
Pitch angle std	-	9.27	10.03	-	10.57	12.25	-	8.32	10.16

Table 2: Results for all load cases (% of reduction)

Conclusions

Comparing all results for the different load cases and control schemes, it can be seen that decentralizing the control loops has a positive effect on the load reduction potential. This is explained due to the large deviations in time and space of the local disturbances and their responses. More detailed load control can be achieved by distributing the control capability. The control design is not necessarily more complicated as soon as no strong couplings are present between the individual loops. Possibly larger reductions can be achieved using information from inflow signals (like in [11]), but normal control approach on the same basis as presented here (possibly in a MIMO framework) has to be used in order to be confirmed where the additional reductions originate.

Such results are considered important for determining preliminary design methodologies for the integration of active aerodynamic devices on wind turbine blades for load reduction. Finally, there are more variables to be explored (optimal sizing, optimal blade and airfoil design, actuator dynamics) but also load cases (extreme loads, emergency events) and safety features.

References

1. Barlas T K, van Kuik G A M. State of the art and prospectives of smart rotor control for wind turbines. *J. Phys.: Conf. Ser.* 2007; 75 012080 (20pp).
2. Troldborg N. Computational study of the Risø B1-18 airfoil with a hinged flap providing variable trailing edge geometry. *Wind Engineering* 2005, 29:89-113.
3. Buhl T, Gaunaa M, Bak C. Load reduction potential using airfoils with variable trailing edge geometry. Proceedings of the 43th AIAA/ASME, Reno, NV, USA, 2005.
4. Buhl T, Gaunaa M, Bak C. Potential load reduction using airfoils with variable trailing edge geometry. *Solar Energy Engineering* 2005, 127:503-16.
5. Andersen P B, Gaunaa M, Bak C, Buhl T. Load alleviation on wind turbine blades using variable airfoil geometry. *Proceedings of the EWEC* 2006, Athens, Greece.
7. Andersen P B, Gaunaa M, Bak C, Buhl T. Wind tunnel test on wind turbine airfoil with adaptive trailing edge geometry. *Proceedings of the 45th AIAA/ASME*, Reno, NV, USA, 2007.
8. Riziotis V A, Voutsinas S G. Aero-elastic modelling of the active flap concept for load control. *Proceedings of the EWEC* 2008, Brussels, Belgium.
9. van Wingerden J-W, Hulskamp A W, Barlas T, Marrant B, van Kuik G A M, Molenaar D-P, Verhaegen M. On the proof of concept of a 'smart' wind turbine rotor blade for load alleviation. *Wind Energy* 2008;11:265–80.

10. Barlas T, van Wingerden J-W, Hulskamp A, van Kuik G. Closed-loop control wind tunnel tests on an adaptive wind turbine blade for load reduction. *Proceedings of the 46th AIAA/ASME*, Reno, NV, USA, 2008.

11. Andersen P B, Henriksen L C, Gaunaa M, Bak C, Buhl T. Integrating deformable trailing edge geometry in modern mega-watt wind turbine controllers, 2008*, Proceedings of the EWEC 2008*, Brussels, Belgium.

12. Snel H. Survey of induction dynamics modelling within BEM-like codes: Dynamic inflow and yawed flow modelling revisited. *Proceedings of the 39th AIAA/ASME*, Reno, NV, USA, 2001.

13. Leishman J G. Unsteady lift of a flapped airfoil by indicial concepts. *Journal of Aircraft* 1994; 31: 288-297

14. Leishman J G. *Principles of helicopter aerodynamics*, 2nd edition, Cambridge aerospace series, 2006.

15. Theodorsen T. General theory of aerodynamic instability and the mechanism of flutter. *NACA Technical Report 497*, 1935.

16. Wagner H. Über die entsehung des dynamischer auftriebes von tragflügeln. *Z. Angew. Math. U. Mech.*, Vol. 118, 1982; 393-409.

17. Bisplinghoff R L, Ashley H, Halfman R L. *Aeroelasticity*. Addison-Wesley Publishing Co.,1955.

18. Molennar D-P. Cost-*effective design and operation of variable speed wind turbines*, PhD Thesis. Delft University Press, 2003.

10. Holierhoek J G. Aeroelasticity of large wind turbines. PhD Thesis. Delft University Press, 2008.

20. Shabana A A. Flexible multibody dynamics: Review of past and recent developments. *Multibody system* dynamics 2001; 1: 189-222.

21. Rauh J, Schiehlen W. Various approaches for the modeling of flexible robot arms. *Proceedings of the Euromech-Colloquium 219 on refined dynamical theories of beams, plates and shells and their applications*.1987; 420-429.

22. Lackner M A, van Kuik g A M. A comparison of msart rotor control approaches using trailing edge flaps and individual pitch control. *Proceedings of the 47th AIAA/ASME*, Orlando, FL, USA, 2009.

23.http://wind.nrel.gov/public/jjonkman/NRELOffshrBsline5MW/NRELOffshrBsline5MW_Onshore.zip (16-02-09).

24. Namik H. Using Simulink[©] and Matllab[©] with FAST. *Internal report*. University of Auckland. June 2008.

25. Simulink[©] Control Design™ 2 – User's guide, The MathWorks Inc. 2008.

26. Bir G, Multi-blade coordinate transformation and its applications to wind turbine analysis. *Proceedings of the 47th AIAA/ASME*, Orlando, FL, USA, 2009.

27. Stol K A, Moll H-G, Birr G, Namik H, A comparison of multi-blade coordinate transformation and direct periodic techniques for wind turbine control design. *Proceedings of the 47th AIAA/ASME*, Orlando, FL, USA, 2009.